

## Lithium Ion Conductors Based on System (Li,Na,La){Ti,Nb,Ta}O with Perovskite Structure

Kobylianska S. D.<sup>1,a</sup>, V'yunov O. I.<sup>1,b</sup>, Belous A.G.<sup>1,c</sup> and Bohnke O.<sup>2,d</sup>

<sup>1</sup>V.I. Vernadskii Institute of General and Inorganic Chemistry of the Ukrainian NAS,  
Palladina Ave 32-34, 03680 Kyiv 142

<sup>2</sup> Institut des Molécules et Matériaux du Mans (UMR 6283 CNRS) Département des Oxydes et  
Fluorures Université du Maine - UFR Sciences et Techniques Avenue Olivier Messiaen 72085  
LE MANS Cedex 9 - France

<sup>a</sup>HUKobylianska\_s@ukr.netUH, <sup>b</sup>HUVyunov@ionc.kiev.uaUH, <sup>c</sup>HUBelous@ionc.kar.netUH,  
<sup>d</sup>HUOdile.Bohnke@univ-lemans.frU

**Keywords:** Titanates, Niobates, Tantalates, Solid-state reactions, Ionic conductivity.

**Abstract.** Solid solutions with defect perovskite structure have been obtained in the systems  $\text{Li}_{0.5-y}\text{Na}_y\text{La}_{0.5}\text{TiO}_3$ ,  $\text{Li}_{0.5-y}\text{Na}_y\text{La}_{0.5}\text{Nb}_2\text{O}_6$  and  $\text{Li}_{0.5-y}\text{Na}_y\text{La}_{0.5}\text{Ta}_2\text{O}_6$  at  $0 \leq y \leq 0.5$ . Their structure has been shown to undergo partial disordering with increasing sodium content in the system  $\text{Li}_{0.5-y}\text{Na}_y\text{La}_{0.5}\text{Nb}_2\text{O}_6$  as in the system  $\text{Li}_{0.5-y}\text{Na}_y\text{La}_{0.5}\text{Ta}_2\text{O}_6$  structure is ordered. Lithium diffusion in systems  $\text{Li}_{0.5-y}\text{Na}_y\text{La}_{0.5}(\text{Nb,Ta})_2\text{O}_6$  exhibits no percolation effects. The ionic conductivity as a function of sodium content in the system  $\text{Li}_{0.5-y}\text{Na}_y\text{La}_{0.5}\text{Nb}_2\text{O}_6$  has a maximum. The ionic conductivity of  $\text{Li}_{0.5-y}\text{Na}_y\text{La}_{0.5}\text{Ta}_2\text{O}_6$  samples decreases with sodium content increase.

### Introduction

Solid-state lithium ion conductors with defect perovskite structure are of great interest. On the one hand, they are model objects for studying the phenomenon of ionic conduction in solids. On the other hand, they can be used as solid electrolytes, electrodes in electrochemical devices. Substituted solid solutions  $\text{Li}_{3x}\text{La}_{2/3-x/3-2x}\text{TiO}_3$  with defect perovskite structure are among the best  $\text{Li}^+$ -ion conducting solid electrolytes (conductivity  $\sigma \sim 10^{-3}$  S/cm at 290 K) [1-3]. The considerable vacancy content and high density of lithium migration channels in the structure of  $\text{Li}_{3x}\text{La}_{2/3-x/3-2x}\text{M}_2\text{O}_6$  ( $\text{M} = \text{Nb, Ta}$ ) defect perovskite solid solutions enabled the fabrication of good lithium ion conductors based on them ( $\sigma \sim 10^{-5}$  to  $10^{-4}$  S/cm at 290 K) [4-7]. At high lithium concentration, conductivity  $\sigma$  in such systems decreases due to the decrease in vacancy ( $\square$ ) content and decrease of so-called bottleneck size [6,8]. The bottleneck size is the narrowest section of the migration channel size, which is formed by 4 corner-shared oxygen octahedra [9] (Fig. 1).

It is known [10] that the size of structural channels depends on the unit-cell volume,  $V$ , which is mainly determined by the ionic radius of A ions of the perovskite structure. Substitutions in A site give the possibility to affect the ionic conductivity of perovskite [4]. It is shown [11,12] that partial substitution of  $\text{La}^{3+}$  ( $r_{\text{CN}=12} = 1.32$  Å) and  $\text{Li}^+$  ( $r_{\text{CN}=6} = 0.74$  Å) by the larger ions  $\text{Sr}^{2+}$  ( $r_{\text{CN}=12} = 1.44$  Å) increases the ionic conductivity of the given materials. Li ions located in A-site of  $\text{Li}_{3x}\text{La}_{2/3-x/3-2x}\text{TiO}_3$ , but not in the centers of oxygen octahedra, that connect contiguous vacant A sites and thus do not block the conduction channel. This fact explains high Li mobility in  $\text{Li}_{0.5}\text{La}_{0.5}\text{TiO}_3$  perovskite, in which vacancies are nominally absent. In the  $(\text{Li}_{1-y}\text{Na}_y)_{0.5}\text{La}_{0.5}\text{TiO}_3$  series,  $\text{Na}^+$  ions like  $\text{La}^{3+}$  ions block the migration channel for Li ions. For  $y > 0.2$ , lithium diffusion in this system follows a percolation mechanism [13]: at this concentration, the conductivity was dropped sharply because the  $\text{Na}^+$  ions block the  $\text{Li}^+$  migration paths.

The systems  $\text{Li}_{0.5-y}\text{Na}_y\text{La}_{0.5}\text{TiO}_3$ ,  $\text{Li}_{0.5-y}\text{Na}_y\text{La}_{0.5}\text{Nb}_2\text{O}_6$  and  $\text{Li}_{0.5-y}\text{Na}_y\text{La}_{0.5}\text{Ta}_2\text{O}_6$  with defect perovskite structure have some structural differences, namely the lanthanum vacancy concentration in  $\text{Li}_{0.5}\text{La}_{0.5}\{\text{Nb,Ta}\}_2\text{O}_6$  systems are considerably higher than in  $\text{Li}_{0.5}\text{La}_{0.5}\text{TiO}_3$  system.

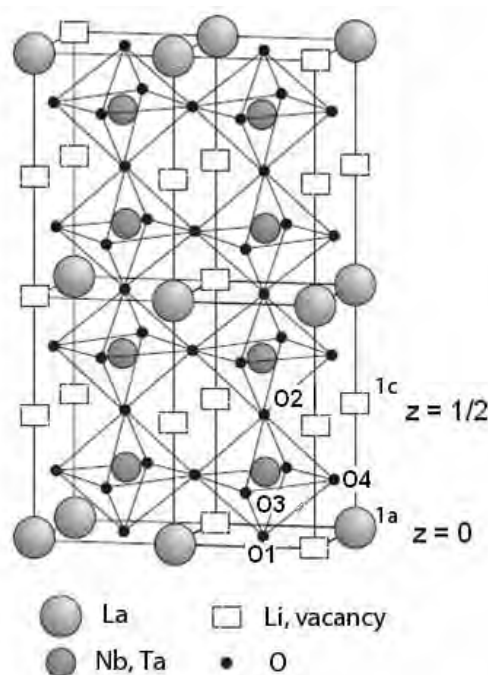


Fig. 1. Crystal structure of  $\text{Li}_{0.5}\text{La}_{0.5}\text{M}_2\text{O}_6$  ( $\text{M} = \text{Nb}, \text{Ta}$ ).

The aim of this work was to elucidate the effect of isovalent substitution of  $\text{Na}^+$  for  $\text{Li}^+$  on the structural properties and ionic conductivity of  $\text{Li}_{0.5-y}\text{Na}_y\text{La}_{0.5}\text{TiO}_3$  and  $\text{Li}_{0.5-y}\text{Na}_y\text{La}_{0.5}(\text{Nb}, \text{Ta})_2\text{O}_6$  ( $0.0 \leq y \leq 0.5$ ).

## Experimental

$\text{Li}_{0.5-y}\text{Na}_y\text{La}_{0.5}\text{TiO}_3$  and  $\text{Li}_{0.5-y}\text{Na}_y\text{La}_{0.5}(\text{Nb}, \text{Ta})_2\text{O}_6$  samples with  $y = 0, 0.1, 0.2, 0.3, 0.4, 0.43, 0.46, 0.48$ , and  $0.5$  were prepared by solid-state reactions. The starting chemicals were  $\text{La}_2\text{O}_3$  (purity > 99.99%, Krasnyi Khimik), extra-pure-grade  $\text{TiO}_2$ ,  $\text{Nb}_2\text{O}_5$  (99.95%, CERAC),  $\text{Ta}_2\text{O}_5$  (99.98%, ALDRICH),  $\text{Li}_2\text{CO}_3$  and  $\text{Na}_2\text{CO}_3$  (99.99%, ALDRICH). The synthesis procedure was similar to that described in detail earlier [2,5,6]. Appropriate powder mixtures were pressed into pellets, which were fired first at 970 K for 4 h (in order to prevent alkali metal losses during heat treatment [14]) and then at 1320 K for 2h, with an intermediate grinding. After homogenization by grinding in a vibratory mill with ethanol, followed by drying, an aqueous 5% solution of polyvinyl alcohol was added as a plasticizer. Green compacts ( $d = 14$  mm,  $p = 80$  MPa) were sintered at temperatures from 1470 to 1720 K for 2 h.

The resultant materials were characterized by X-ray diffraction (XRD). XRD patterns were collected on a DRON-4-07 powder diffractometer ( $\text{CuK}\alpha$  radiation). Structural parameters were determined by the Rietveld full-profile analysis method using XRD data.

In electrical measurements, we used samples 12mm in diameter and 1mm in thickness. Pt electrodes ( $0.5 \mu\text{m}$ ) were deposited by electron-beam evaporation. The impedance of our samples was measured from 100 Hz to 1 MHz with a Solartron Analytical 1260A impedance/gain phase analyzer. The electrical equivalent circuit and its components were identified using the Frequency Response Analyser 4.7 program. The electrical conductivity ( $\sigma$ ) was measured in dry air.

## Results and discussion

XRD showed (Fig. 2) that irrespective of the sodium content, the sintered materials were single-phase and had an rhombohedral (space group  $R\bar{3}c$ ) for  $\text{Li}_{3x}\text{La}_{2/3-x1/3-2x}\text{TiO}_3$  [15] and orthorhombic (space group  $Pmmm$ ) for  $\text{Li}_{3x}\text{La}_{2/3-x4/3-2x}(\text{Nb}, \text{Ta})_2\text{O}_6$  defect perovskite structure. In the system  $\text{Li}_{0.5-y}\text{Na}_y\text{La}_{0.5}\text{TiO}_3$  we observed the 101 superlattice reflections at  $2\theta = 25.6$  and  $18.5^\circ$ , which indicates the appearance of the tetragonal crystal system  $\text{Li}_{3x}\text{La}_{2/3-x1/3-2x}\text{TiO}_3$  (space group  $Pbmn$ ) and the ordering of cation vacancies in  $c$  directions (Fig. 2a) [16]. It is known [17] that for system

$\text{Li}_{3x}\text{La}_{2/3-x}\square_{1/3-2x}\text{TiO}_3$  at low lithium content ( $x \leq 0.1$ )  $\text{La}^{3+}$  ions are located in the plane  $z = 0$ , where the site occupations is 91%, while in the plane  $z = 1/2$  the site occupations is 33%. With increasing concentration of lithium in  $\text{Li}_{3x}\text{La}_{2/3-x}\square_{1/3-2x}\text{TiO}_3$  intensity XRD reflection of last plane decreases. This is due to disordering in the planes  $z = 1/2$  and  $z = 0$ , i.e. uniform distribution of La and cation vacancies in both planes [18]. Lowering of the intensity and broadening of superstructure reflections in the system  $\text{Li}_{0.5-y}\text{Na}_y\text{La}_{0.5}\text{TiO}_3$  with increasing  $y$  are due to a decrease in the content of phase with orthorhombic symmetry which is characteristic of the original  $\text{Li}_{0.5}\text{La}_{0.5}\text{TiO}_3$ . The intensity of the peaks at  $2\theta = 25.6$  and  $18.5^\circ$  decreases with increasing temperature and time of heat treatment [13]. Over the entire range of isovalent substitutions in the systems  $\text{Li}_{3x}\text{La}_{2/3-x}\square_{4/3-2x}(\text{Nb,Ta})_2\text{O}_6$  studied, we observed the 101 superlattice reflection.

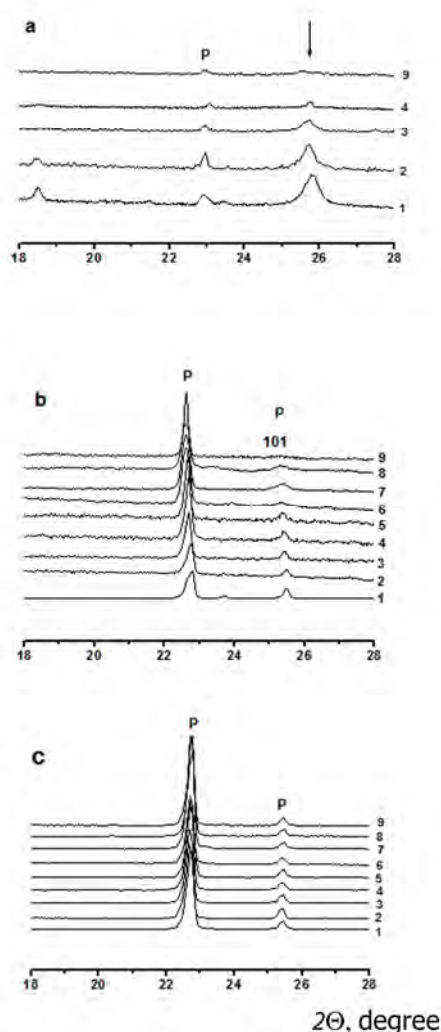


Fig. 2. XRD patterns of sintered  $\text{Li}_{0.5-x}\text{Na}_y\text{La}_{0.5}\text{TiO}_3$  (a),  $\text{Li}_{0.5-y}\text{Na}_y\text{La}_{0.5}\square\text{Nb}_2\text{O}_6$  (b) and  $\text{Li}_{0.5-y}\text{Na}_y\text{La}_{0.5}\text{Ta}_2\text{O}_6$  (c) samples with  $y = 0$  (1); 0.1 (2); 0.2 (3); 0.3 (4); 0.4 (5); 0.43 (6); 0.46 (7); 0.48 (8); 0.5 (9).

It is known that for  $\text{La}_{2/3-x}\square_{4/3}(\text{Nb,Ta})_2\text{O}_6$  structure (Fig. 1) in the plane  $z = 0$  there are vacancies and lanthanum ions, and in the plane  $z = 1/2$  only vacancies [19]. Ordering of vacancies in these planes is confirmed by the presence of 101 superstructure reflections at  $2\theta = 25.5^\circ$ . In the system  $\text{Li}_{0.5-y}\text{Na}_y\text{La}_{0.5}\square\text{Nb}_2\text{O}_6$  with increasing  $y$  superstructure reflections become lower and wider, which may be interpreted as the filling of vacancies and the partial ordering of cation vacancies. This may indicate a preferential substitution of alkali metal ions in the plane  $z = 1/2$ .

At the same time in the system  $\text{Li}_{0.5-y}\text{Na}_y\text{La}_{0.5}\square\text{Ta}_2\text{O}_6$  the intensity of superstructure reflection 101 at  $2\theta = 25.5^\circ$  with an increase  $y$  remain unchanged (Fig. 2c). This can be explained by the fact that in these materials there is considerable loss of alkali ions due to the high temperature sintering of ceramics (1670-1760 K). This leads to the fact that alkali metal ions are located preferentially in the plane  $z = 0$ . In the plane  $z = 1/2$ , the vacancies concentration does not change during the substitution.

It should be noted that the losses of lithium ions in niobium- and titanium-containing materials are significantly lower compared to the tantalum-containing ones. This is due to the lower ceramics sintering temperature (1570 and 1470 K respectively).

The table 1,2 present the structural parameters of  $\text{Li}_{0.5-y}\text{Na}_y\text{La}_{0.5}\square(\text{Nb,Ta})_2\text{O}_6$  with various sodium content. The parameters in the structure of  $\text{La}_{2/3-x}\square_{4/3-2x}\text{M}_2\text{O}_6$  were used as initial [19]. The unit-cell volume increases with sodium content, according to Vegard's law in all systems (Fig. 3) because the ionic radius of sodium is greater than that of lithium.

Table 1.

Unit-cell parameters, atomic position coordinates, and agreement factors for  $\text{Li}_{0.5-y}\text{Na}_y\text{La}_{0.5}\square\text{Nb}_2\text{O}_6$ 

| Unit cell parameters, atomic position coordinates, and agreement factors for $\text{La}_{0.5-\text{y}}\text{Pr}_{\text{y}}\text{Al}_{0.5}\text{Fe}_{1.5}\text{Nb}_2\text{O}_{10}$ |                |           |           |                    |       |                  |
|---|----------------|-----------|-----------|--------------------|-------|------------------|
| $y$   | a              | b         | c         | $V [\text{\AA}^3]$ | $R_B$ | $R_{\text{exp}}$ |
|   | $[\text{\AA}]$ |           |           |                    | [%]   |                  |
| 0.0   | 3.002(1)       | 3.005(2)  | 7.8521(2) | 119.452(6)         | 9.14  | 6.98             |
| 0.1   | 3.903(8)       | 3.904(7)  | 7.854(2)  | 119.7(3)           | 6.42  | 8.62             |
| 0.2   | 3.906(8)       | 3.907(8)  | 7.852(1)  | 119.8(4)           | 6.98  | 9.15             |
| 0.3   | 3.915(1)       | 3.912(1)  | 7.861(1)  | 120.40(5)          | 5.92  | 9.78             |
| 0.4   | 3.915(9)       | 3.915(9)  | 7.861(1)  | 120.5(2)           | 5.36  | 8.36             |
| 0.43  | 3.923(1)       | 3.9311(6) | 7.850(2)  | 121.07(5)          | 7.36  | 5.01             |
| 0.46  | 3.918(1)       | 3.923(1)  | 7.860(2)  | 120.79(6)          | 6.30  | 4.84             |
| 0.48  | 3.9167(8)      | 3.9304(7) | 7.846(2)  | 120.78(4)          | 5.94  | 4.18             |
| 0.5   | 3.925(1)       | 3.9278(6) | 7.848(3)  | 120.98(6)          | 6.40  | 8.96             |

Note: Positions of atoms and vacancies: La (1a), 0 0 0; Nb (2t), 1/2 1/2 z; O1 (1f), 1/2 1/2 0; O2 (1h), 1/2 1/2 1/2; O3 (2s), 1/2 0 z; O4 (2r), 0 1/2 z;  $\square$  (1c), 0 0 1/2.

Table 2.

Unit-cell parameters, atomic position coordinates, and agreement factors for  $\text{Li}_{0.5-y}\text{Na}_y\text{La}_{0.5}\square\text{Ta}_2\text{O}_6$ 

| y    | a                | b         | c         | V [ $\text{\AA}^3$ ] | R <sub>B</sub> | R <sub>exp</sub> |
|------|------------------|-----------|-----------|----------------------|----------------|------------------|
|      | [ $\text{\AA}$ ] |           |           |                      | [%]            |                  |
| 0.0  | 3.902(2)         | 3.903(2)  | 7.8533(4) | 119.54(8)            | 21.6           | 20.9             |
| 0.1  | 3.9067(9)        | 3.905(1)  | 7.8525(4) | 119.81(4)            | 17.5           | 11.4             |
| 0.2  | 3.911(1)         | 3.911(1)  | 7.8663(4) | 120.31(5)            | 11.0           | 8.08             |
| 0.3  | 3.911(1)         | 3.911(1)  | 7.8751(4) | 120.47(5)            | 20.0           | 13.1             |
| 0.4  | 3.915(1)         | 3.915(1)  | 7.8757(1) | 120.71(5)            | 26.6           | 20.1             |
| 0.46 | 3.9167(7)        | 3.9159(7) | 7.8809(2) | 120.87(3)            | 11.4           | 7.81             |
| 0.48 | 3.916(2)         | 3.916(2)  | 7.8811(2) | 120.88(8)            | 11.0           | 7.84             |
| 0.5  | 3.917(2)         | 3.918(2)  | 7.8785(3) | 120.90(9)            | 13.4           | 9.84             |

Note: Positions of atoms and vacancies: La (1a) 0 0 0; Ta (2t) 1/2 1/2 z; O1 (1f) 1/2 1/2 0; O2 (1h) 1/2 1/2 1/2; O3 (2s) 1/2 0 z; O4 (2r) 0 1/2 z;  $\square$  (1c) 0 0 1/2.

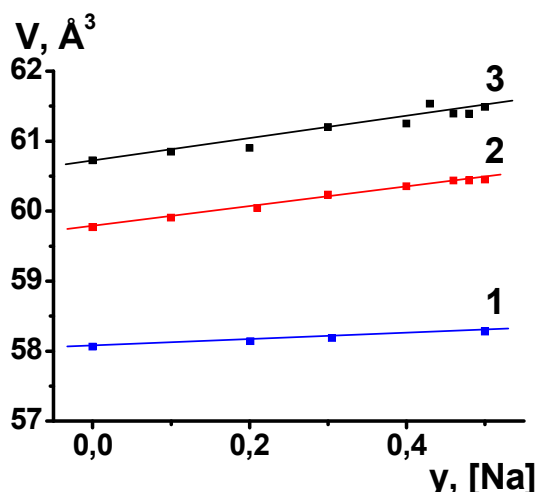


Fig. 3. Unit-cell volume as a function of sodium content for  $\text{Li}_{0.5-x}\text{Na}_x\text{La}_{0.5}\text{TiO}_3$  (1) [15],  $\text{Li}_{0.5-y}\text{Na}_y\text{La}_{0.5}\square\text{Ta}_2\text{O}_6$  (2) and  $\text{Li}_{0.5-y}\text{Na}_y\text{La}_{0.5}\square\text{Nb}_2\text{O}_6$  (3).

The large  $\text{Na}^+$  ions do not participate in ionic transport in systems investigated [20], and the ionic conductivity are determined only by  $\text{Li}^+$  transport. Fig. 4 shows that the nature of the lithium conductivity as a function of sodium content in these systems is different. In the system  $\text{La}_{0.5}\text{Li}_{0.5-y}\text{Na}_y\text{TiO}_3$ , the conductivity is changed only slightly with increasing  $y$  up to  $y = 0.1$ , and decreased sharply (by 5 - 6 orders of magnitude) above this sodium content (Fig. 4, curve 1). This is because the sodium ions block the  $\text{Li}^+$  migration paths [20]. In this system the conductivity is described by the percolation model of lithium diffusion [11].

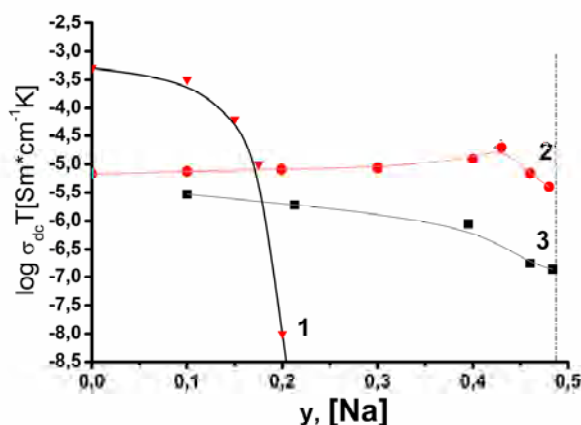


Fig. 4. Conductivity as a function of sodium content for  $\text{Li}_{0.5-x}\text{Na}_x\text{La}_{0.5}\text{TiO}_3$  (1) [15],  $\text{Li}_{0.5-y}\text{Na}_y\text{La}_{0.5}\square\text{Nb}_2\text{O}_6$  (2),  $\text{Li}_{0.5-y}\text{Na}_y\text{La}_{0.5}\square\text{Ta}_2\text{O}_6$  (3) at 290 K.

In systems  $\text{Li}_{3-x}\text{La}_{2/3-x}\square_{4/3-2x}(\text{Nb,Ta})_2\text{O}_6$  another character of the conductivity is observed (Fig. 4, curves 2,3). In the niobium-containing system, substitution of sodium for lithium increases conductivity with a maximum at  $y = 0.43$ . Further increase in  $\text{Na}^+$  content leads to a decrease in conductivity. Lithium ion diffusion in the  $\text{Li}_{0.5-y}\text{Na}_y\text{La}_{0.5}\square\text{Nb}_2\text{O}_6$  system exhibits no percolation effects. Samples of this system contain a significant number of structural vacancies for any  $\text{Li}/\text{Na}$  ratio. The ionic conductivity of  $\text{Li}_{0.5-y}\text{Na}_y\text{La}_{0.5}\square\text{Nb}_2\text{O}_6$  at substitution of sodium for lithium increases from  $\sigma = 6.85 \times 10^{-6}$  S/cm at  $y = 0$  to  $1.28 \times 10^{-5}$  S/cm at  $y = 0.43$  (Fig. 4, curve 2). Such concentration dependence of conductivity can be attributed to two competing factors. It is known that the conductivity  $\sigma$  is proportional to the concentration of charge carriers,  $n$ , their mobility,  $\mu$  and charge,  $q$ , namely  $\sigma = n \times \mu \times q$ . In the range  $0 \leq y \leq 0.43$ , the concentration of charge carriers (lithium ions) decreases. However, unit cell volume is increased with  $y$  (Fig. 3). As a consequence,

the sizes of structural channels and the mobility of lithium ions are increased. In the range ( $0 \leq y \leq 0.43$ ), the increase of lithium ions mobility leads to the increase of conductivity. However, at  $y > 0.43$ , the charge carriers (lithium ions) become too little and conductivity decreases.

In  $\text{Li}_{0.5-y}\text{Na}_y\text{La}_{0.5}\square\text{Ta}_2\text{O}_6$  system, the conductivity of sample decreases with increase of sodium content from  $\sigma = 2.06 \times 10^{-5}$  S/cm at  $y = 0$  to  $6.4 \times 10^{-7}$  S/cm at  $y = 0.48$  (Fig. 4, curve 3). The difference between conductivity of Nb- and Ta-containing systems occurs due to different lithium losses during sintering. Ceramics  $\text{Li}_{0.5-y}\text{Na}_y\text{La}_{0.5}\square\text{Ta}_2\text{O}_6$  were sintered at  $\sim 1750$  K that is 150-200 K higher than  $\text{Li}_{0.5-y}\text{Na}_y\text{La}_{0.5}\square\text{Nb}_2\text{O}_6$ . Higher lithium losses from Ta-containing samples lead to the fact that increasing in unit cell with  $y$  has no positive effect on the conductivity.

## Conclusions

The present results demonstrate that  $\text{Li}_{0.5-y}\text{Na}_y\text{La}_{0.5}\text{TiO}_3$  and  $\text{Li}_{0.5-y}\text{Na}_y\text{La}_{0.5}\square(\text{Nb,Ta})_2\text{O}_6$  systems have a defect perovskite structure (rhombohedral, sp. gr.  $R\bar{3}c$  and tetragonal symmetry, sp. gr. Pmmm) in the range of  $0 < y \leq 0.5$ . The ionic conductivity in the systems  $\text{Li}_{0.5-y}\text{Na}_y\text{La}_{0.5}\square(\text{Nb,Ta})_2\text{O}_6$  unlike shown earlier  $\text{Li}_{0.5-y}\text{Na}_y\text{La}_{0.5}\text{TiO}_3$ , is not described by percolation model. The ionic conductivity of  $\text{Li}_{0.5-y}\text{Na}_y\text{La}_{0.5}\square\text{Nb}_2\text{O}_6$  as a function of sodium content has a maximum due to two competing factors: the increase in perovskite unit cell volume and the decrease in lithium ion concentration. In the  $\text{Li}_{0.5-y}\text{Na}_y\text{La}_{0.5}\square\text{Ta}_2\text{O}_6$  system, the ionic conductivity as a function of sodium content decreases due to significant loss of lithium during sintering of ceramics.

## References

- [1] A.G. Belous, V.I. Butko, G.N. Novitskaya, et al., Electrical Conductivity of  $\text{La}_{2/3-x}\text{M}_{3x}\text{TiO}_3$  Perovskites, Ukr. Fiz. Zh. (Russ. Ed.) 31 (1986) 576-581.
- [2] A.G. Belous, Properties of Heterosubstituted Titanates with Perovskite Structure, 3rd Euro Ceramics 2 (1993) 341-346.
- [3] J. Ibarra, A. Varez, C. Leon, et al., Influence of Composition on the Structure and Conductivity of the Fast Ionic Conductors  $\text{La}_{2/3-x}\text{Li}_{3x}\text{TiO}_3$  ( $0.03 \leq x \leq 0.167$ ), Solid State Ionics 134 (2000) 219-228.
- [4] O. N. Gavrilenko, A. G. Belous, L. L. Kovalenko, Ye. V. Pashkova, Effect of the A-site substitution on the structure peculiarities and ionic conductivity of solid electrolytes  $\text{La}_{2/3-x-y}\text{Li}_{3x-y}\text{Sr}_{2y/3-2x}\text{Nb}_2\text{O}_6$ . Mater. Manuf. Process 23 (2008) 607-610.
- [5] A.G. Belous, E.B. Novosadova, I.R. Diduh et al., Formation of cationic conductivity in complex niobium containing materials with defect perovskite structure, Ionic melts and electrolytes (Russ. Ed.) 4 (1986) 68-73.
- [6] O. Bohnke, The fast lithium-ion conducting oxides  $\text{Li}_{3x}\text{La}_{2/3-x}\text{TiO}_3$  from fundamentals to application, Solid State Ionics 179 (2008) 9-15.
- [7] A. Belous, E. Pashkova, O. Gavrilenko et al., Solid electrolytes based on lithium-containing lanthanum metaniobates, J. Eur. Ceram. Soc. 24 (2004) 1301-1304.
- [8] A. Belous, E. Pashkova, O. Gavrilenko et al., Lithium ion-conducting materials based on complex metaniobates and metatantalates  $\text{La}_{2/3-x}\text{Li}_{3x}\square_{4/3-2x}[\text{Nb}]\text{Ta}_2\text{O}_6$  with defect-perovskite structure, Ionics 9 (2003) 21-27.
- [9] O.N. Gavrilenko, A.G. Belous, E.V. Pashkova and V.N. Mirnyi, Structural and Transport Properties of  $\text{La}_{2/3-x}\text{Li}_{3x}\square_{4/3-2x}\text{Ta}_2\text{O}_6$  Perovskite-Like Solid Solutions, Inorg. Mater. 38 (2002) 949-953.
- [10] M. Itoh, Y. Inaguma, W. Jung et al., High lithium ion conductivity in the perovskite-type compounds  $\text{Ln}_{1/2}\text{Li}_{1/2}\text{TiO}_3$ , (Ln = La, Pr, Nd, Sm), Solid State Ionics 70/71 (1995) 203-207.

- 
- [11] A. Rivera, C. Leon, J. Santamaria, et al., Percolation-Limited Ionic Diffusion in  $\text{Li}_{0.5-x}\text{Na}_x\text{La}_{0.5}\text{TiO}_3$  Perovskites ( $0 \leq x \leq 0.5$ ), Chem. Mater. 14 (2002) 5148-5152.
  - [12] M. Sanjuan, M. Laguna, A. Belous, and O. V'yunov, On the Local Structure and Lithium Dynamics of  $\text{La}_{0.5}(\text{Li},\text{Na})_{0.5}\text{TiO}_3$  Ionic Conductors. A Raman Study, Chem. Mater. 17 (2005) 5862-5866.
  - [13] J. Sanz, A. Rivera, C. León et al., Li mobility in  $\text{La}_{0.66-y/3}(\text{Li},\text{Na})_y\text{TiO}_3$  ( $0.09 \leq x \leq 0.5$ ). A modes system for the percolation theory, Mater. Res. Soc. Publications 756 (2003) EE2.31 - EE2.36.
  - [14] A.G. Belous, O.N. Gavrilenko, E.V. Pashkova, and V.N. Mirnyi, Lithium Ion Conductivity and Crystal-Chemical Aspects of  $\text{La}_{2/3-x}\text{Li}_{3x}\text{Nb}_{4/3-2x}\text{O}_6$  Defect Perovskite Solid Solutions, Elektrokhimiya 38 (2002) 479-484.
  - [15] C.P. Herrero, A. Varez, A. Rivera et al., Influence of Vacancy Ordering on the Percolative Behavior of  $(\text{Li}_{1-x}\text{Na}_x)_{3y}\text{La}_{2/3-y}\text{TiO}_3$  Perovskites, J. Phys. Chem. B 109 (2005) 3262-3268.
  - [16] R. Jimenez, A. Varez, J. Sanz, Influence of octahedral tilting and composition on electrical properties of the  $\text{Li}_{0.2-x}\text{Na}_x\text{La}_{0.6}\text{TiO}_3$  ( $0 \leq x \leq 0.2$ ) series, Solid State Ionics 179 (2008) 495-502.
  - [17] J. Ibarra, A. Varez, C. Leon et al., Influence of composition on the structure and conductivity of the fast ionic conductors  $\text{La}_{2/3-x}\text{Li}_{3x}\text{TiO}_3$  ( $0.03 \leq x \leq 0.167$ ), Solid State Ionics 134 (2000) 219-228.
  - [18] A. Rivera, C. Leon, J. Santamaria et al.,  $\text{Li}_{3x}\text{La}_{2/3-x}\text{TiO}_3$  fast ionic conductors. Correlation between lithium mobility and structure, J. Non-Cryst. Solids 307-310 (2002) 992-998.
  - [19] V.B. Nalbandyan, and I.A. Shukaev, Novel tantalate and niobate, Zh. Neorg. Khim. (Russ. Ed.) 34 (1989) 793-795.
  - [20] R. Jimenez, A. Rivera, A. Varez, and J. Sanz, Li mobility in  $\text{Li}_{0.5-x}\text{Na}_x\text{La}_{0.5}\text{TiO}_3$  perovskites ( $0 \leq x \leq 0.5$ ). Influence of structural and compositional parameters, Solid State Ionics. 180 (2009) 1362-1371.